

A Simple and Practical Design Approach to Realize Band-Pass Photonic Crystal Fiber Filters

Shailendra K. Varshney, Kunimasa Saitoh, Nikolaos J. Florous, and Masanori Koshiba

Division of Media and Network Technologies, Hokkaido University, Sapporo 060-0814, Japan

E-mail: skvarshney_10@yahoo.co.uk

A new in-line photonic crystal fiber band-pass filter based on a simple design approach with more than 76% transmission, centered at 1136 nm, is numerically investigated. A beam-propagation-method was used to verify the operation of filter.

1. Introduction

Wavelength selective devices such as optical band-pass or band-rejection filters are in great demand for wavelength division multiplexing (WDM) or dense-WDM (DWDM) optical fiber communication systems. Such devices can serve as building blocks for all-optical channel selection. Several types of all-fiber spectral filters have been reported during the last decade [1-2]. Among them, filters constructed with fused-taper couplers, dissimilar fiber couplers, and dual-core fibers have received much attention. On the other hand, photonic crystal fibers (PCFs) have been a subject of intensive research due to their novel optical properties such as ultra-wide band single mode operation [3]. PCFs can provide elegant ways to act as functional devices such as, narrow band pass filters based on solid and hollow core photonic crystal fibers and polarization independent couplers [4-6].

Most of the PCF designs were based on dual core separated by a resonator. The biggest disadvantage of such functional devices is their practical realization as they may show difficulty in the fabrication due to complex geometry in the cladding. Therefore, to realize a feasible structure, we have adopted a simpler design approach to achieve PCF band-pass filter. Our design procedure is based on the fusion of two different physical mechanisms [7] that is short-wavelength cut-off (long-wavelength band-pass filter) and long wavelength cut-off (short wavelength band-pass filter) of the fundamental mode. The short wavelength cut-off of the fundamental mode is achieved by doping the core with fluorine material of lower refractive index [8], while the long wavelength cut-off is obtained by increasing the size of the air-holes in the first ring. This will impart a band-pass filter behavior to PCFs. The fiber's geometrical parameters as well as the doping concentration and doping size play an

important role in determining the optimum performance of the device.

2. Fiber's profile and design principle

Figure 1 shows the transverse cross-section of the proposed fiber filter. The doping region (red circle) is characterized by doping size D and fluorine concentration Δ (%). The air-holes surrounding the doped region have diameter d' while the rest of air-holes have hole-diameters d . The design parameters are $d = 0.90 \mu\text{m}$ and $\Lambda = 3.2 \mu\text{m}$ and the index of silica was assumed 1.458 in calculations. This PCF presents an anti-guiding wavelength [8] which is simply a short-wavelength cut-off and thus the fiber allows all longer wavelengths larger than the anti-guiding wavelength and hence the device can act as a long wavelength-pass filter. By increasing the size of the air-holes fencing the fluorine-doped region, a long-wavelength cut-off can be achieved where the index of the guided mode becomes smaller than the index of the cladding mode and therefore the fiber can work as a short-wavelength pass filter. Therefore, the proposed PCF device can operate as a band-pass filter. The 3-dB bandwidth can be controlled by manipulating the geometrical parameters. We have employed a full-vectorial finite element method and beam propagation method (BPM) [9] to simulate the modal characteristics and transmission response of the PCF based band-pass filter.

For the present analysis, we have considered two sets of simulation parameters where the total number of air-hole rings N , size of doping region, and doping concentration were varied, while other design parameters such as pitch, hole diameters d and d' are fixed. Figure 2(a) depicts the spectral variation of the absolute difference between the index of the fundamental guided core mode n_{eff} and the effective cladding index n_{cl} , while the inset graph shows the index variation of these two, where $d' = 1.24 \mu\text{m}$, $D = 3.2 \mu\text{m}$, and $\Delta = 0.16 \%$. It can be seen from the graph that the index of the guided mode matches at two different wavelengths, that is short and longer wavelengths, respectively, as presented by arrows in Fig. 2(a). This establishes the band-pass filtering operation of the proposed PCF. Both short and long-

wavelength cut-off can be tailored by changing the hole diameter d and d' . In addition, if we increase Δ , the fiber may not guide the fundamental mode and it becomes leaky, whereas if we decrease Δ , the short-wavelength cut-off shifts to shorter side and long-wavelength cut-off shifts towards longer wavelength for a particular set of geometrical parameters. Next, we run the BPM solver for the design parameters as mentioned in Table 1. Figure 2(b) shows the transmission characteristics of the device for two sets of parameters. The solid red-curve corresponds to the case where the doping radius is half of the pitch, fluorine concentration is 0.16 % ($n_f = n_{si} - \Delta$), and total number of air-hole rings are eight. It is seen that the insertion loss (IL) is 2.2 dB while the 3-dB bandwidth is 385 nm when the PCF is 5 cm long. The 3-dB bandwidth decreases when the length of fiber increases at the cost of higher insertion loss. This is due to the fact that the operation of the device relies on the leakage loss characteristics of the fiber. The fiber is very leaky near the cut-off wavelengths, thus we observe a trade-off between the 3-dB bandwidth and the length of the fiber. Next, we analyze the scenario where the doping concentration is increased and the doping radius is reduced to 1 μm in order to compensate for the reduced doping index (solid blue curve). An insertion loss of 2.8 dB and 307 nm of 3-dB bandwidth can be obtained when the fiber length was 8 cm. The insertion loss comes from the mismatch of the mode-fields that can be understood as an optical mode field from the unperturbed PCF (when $d'=d$) without fluorine doping is launched to the proposed PCF filter.

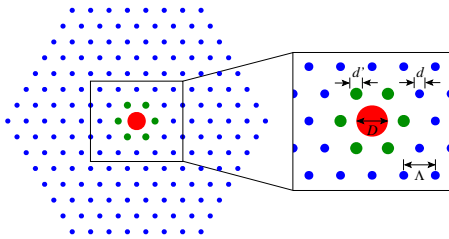


Fig. 1 Schematic representation of the proposed PCF band-pass filter, the core is doped with fluorine material as shown by red circle with doping size D , the size of the first six air-holes is increased to d' from d , and the lattice constant is Λ .

Table 1. Fiber design parameters

Parameters	d'/Λ	d/Λ	r_d	Δ	N
Set-1	0.387	0.28	1.6 mm	0.16 %	8
Set-2	0.387	0.28	1.0 mm	0.35 %	11

3. Summary

The band-pass filtering characteristics of solid core PCFs have been obtained through a simple and easy

to fabricate design approach which was based on a W-type index profile with a depressed core. The basic physical insight in the operation of the device was the control of the leakage loss property of the fundamental mode. It has been found that the controlled variation of the fiber's structural parameters, namely doping radius, doping level, and first ring's hole-diameters, the band pass characteristics of PCFs can be tuned and such study as well as the thermo-optical properties of the device is currently under investigation and will be reported in the conference.

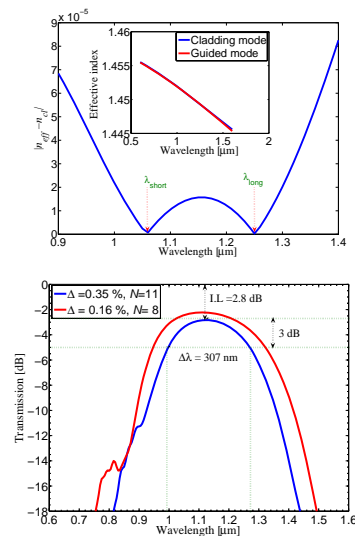


Fig.2. (a) Spectral variation of the absolute difference between the indices of the cladding and fundamental guided mode, inset shows the effective index variation of the cladding (solid blue curve) and guided mode (solid red curve), (b) Transmission characteristics of a 5 cm (solid red curve) and an 8 cm (solid blue curve) long PCF band pass filter. It can be clearly seen that the fiber corresponding to Set-2, shows a 3-dB bandwidth of 307 nm with more than 76 % transmittance as calculated by BPM solver and exhibits an insertion loss of approximately 2.8 dB.

References

- [1] C. Chung and A. Safaai-Jazi, J. Lightwave Technol. **10**, 42-45 (1992).
- [2] R. Zengerle and O.G. Leminger, J. Lightwave Technol. **LT-5**, 1196-1198 (1987).
- [3] T.A. Birks, J.C. Knight, and P.St. J. Russell, Opt. Lett. **22**, 961-963 (1997).
- [4] K. Saitoh, N.J. Florous, and M. Koshiba, Opt. Express **13**, 10327-10335 (2005).
- [5] J.M. Fini, R.T. Bise, M.F. Yan, A.D. Yablon, and P. W. Wisk, Opt. Express **13**, 10022-10033 (2005).
- [6] N.J. Florous, K. Saitoh, T. Murao, M. Koshiba, and M. Skorobogatiy, Opt. Express **14**, 4861-4872 (2006).
- [7] K. Morishita, J. Lightwave Technol. **7**, 198-201 (1989).
- [8] B.J Mangan, J. Arriaga, T.A. Birks, J.C. Knight, and P.St.J. Russell, Opt. Lett. **26**, 1469-1471 (2001).
- [9] K. Saitoh and M. Koshiba, IEEE J. Quantum Electron. **38**, 927-933 (2002).